

One-dimensional uranium–organic coordination polymers: crystal and electronic structures of uranyl-diacetohydroxamate†Philippe F. Weck,^{*a} Cynthia-May S. Gong,^a Eunja Kim,^b Pierre Thuéry^c and Kenneth R. Czerwinski^a

Received 18th February 2011, Accepted 30th March 2011

DOI: 10.1039/c1dt10267b

The structure of the uranyl-diacetohydroxamate compound, $\text{UO}_2(\text{C}_2\text{NO}_2\text{H}_4)_2$, was elucidated using a combination of single crystal X-ray diffraction measurements and all-electron scalar relativistic density functional calculations. This polymeric compound crystallizes in the $C2/c$ space group (IT No. 15; $a = 12.8386(13)$ Å, $b = 7.5661(7)$ Å, $c = 8.9299(9)$ Å, $\beta = 103.185(2)^\circ$; $Z = 4$), with main-chain repeating units featuring a bidentate structure analogous to that frequently found for d-block as well as lanthanide metal ions. Density functional analysis reveals that this compound is a semiconductor, with a direct band gap of 1.1 eV.

Introduction

As the simplest geometric arrangement in metal–organic coordination polymers, one-dimensional assemblies have been widely investigated and, while their structural intricacy is limited, some of them display interesting properties, particularly magnetic, electric and optical.¹ Among the reported coordination polymers and frameworks including f elements, those involving actinide ions are less numerous than those with lanthanide ions, and they are mainly limited to uranyl ion complexes, but this domain of uranyl–organic assemblies has undergone a rapid development in recent years.² The geometric requirements of the linear uranyl cation, which is generally surrounded by four to six donor atoms in its equatorial plane, endow this ion with a particular propensity to form planar coordination polymers, either two-dimensional, or one-dimensional with a ribbon shape. Numerous examples of these geometries obtained with carboxylate ligands have been known,³ and many novel cases of one-dimensional polymers have recently been reported with ligands as diverse as polycarboxylates,⁴ carboxyphosphonates⁵ or squarate.⁶ Although hydroxamates are interesting ligands in this context, since they are potentially both chelating and bridging, they have been little used in combination with actinide ions and in particular with uranyl ions. A search of the Cambridge Structural Database (CSD, version 5.32)⁷ gives only five crystal structures of uranyl–hydroxamate complexes, three of which involve the bis-phenyl-substituted *N*-phenyl-

benzohydroxamate,⁸ and the others are either 4-isopropylphenyl-benzohydroxamate,⁹ or 2-hydroxy-benzohydroxamate.¹⁰ All these compounds are molecular species, except for the latter, which is polymeric. In the molecular case, the uranyl ion is bound to either one^{8a} or two^{8b,c,9} hydroxamate molecules. Further work on these complexes is all the more desirable given that hydroxamic acids are candidates for processing in advanced nuclear fuel cycles.¹¹ An original, dry synthesis of the uranyl-diacetohydroxamate complex has been reported, together with its characterization by various methods (UV-Vis and FT-IR spectroscopy, ¹H NMR, EXAFS, and fluorescence).¹¹ It has now been possible to determine the crystal structure of this complex by single-crystal X-ray diffraction. This result is reported herein, together with all-electron scalar relativistic density functional calculations which permitted the determination of the electronic band structure of the complex.

Results and discussion**Structural features of U-AHA**

The uranyl-diacetohydroxamate (U-AHA) polymeric compound crystallizes in the $C2/c$ space group, with main-chain repeating units featuring a bidentate structure analogous to that frequently found for d-block as well as lanthanide metal ions, as can be seen from the CSD.⁷ The structure of U-AHA consists of the ubiquitous uranyl unit positioned with uranium on a $\bar{1}$ site and coordinated by six equatorial oxygen atoms donated by four symmetry-related acetohydroxamic acid molecules (Fig. 1). The local environment of the uranium metal center is hexagonal bipyramidal with two short axial $\text{U}=\text{O}$ bonds, both at a distance of 1.766(5) Å and a linear $\text{O}=\text{U}=\text{O}$ angle, and with the six equatorial oxygen atoms forming a plane with a rms deviation of 0.248 Å. The hydroxamate ligand forms a five-membered chelate ring with the uranium atom (rms deviation of the mean plane 0.171 Å). Both acidic oxygens are unique and exist in different bonding environments; while the carbonyl oxygen atom O2 is monodentate, the hydroxamate atom

^aDepartment of Chemistry and Harry Reid Center for Environmental Studies, University of Nevada-Las Vegas, Las Vegas, NV, 89154, USA. E-mail: weckp@unlv.nevada.edu; Fax: (702) 895-4072; Tel: (702) 895-1159

^bDepartment of Physics and Astronomy, University of Nevada-Las Vegas, Las Vegas, NV, 89154, USA

^cCEA, DSM/IRAMIS, UMR 3299 CEA/CNRS SIS2M, 91191, Gif-sur-Yvette, France

† CCDC reference number 814702. For crystallographic data in CIF or other electronic format see DOI: 10.1039/c1dt10267b

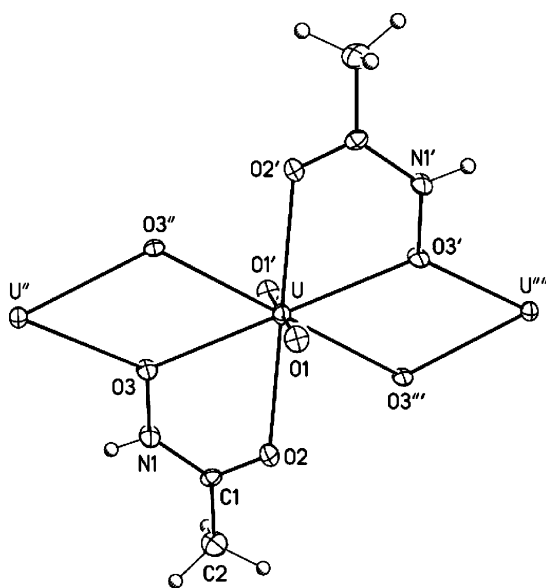


Fig. 1 View of the U-AHA complex with displacement ellipsoids drawn at the 50% probability level. Symmetry codes: ' = 1 - x, -y, 2 - z; '' = 1 - x, y, 5/2 - z; ''' = x, -y, z - 1/2; '''' = 1 - x, y, 3/2 - z.

O3 is μ_2 -bridging between two symmetry-related uranium metal centers. The end result of this bonding pattern is an extended chain structure propagating along the *c*-axis (Fig. 2), which is analogous to that obtained with 2-hydroxy-benzohydroxamate, with the bridging oxygen atom being that bound to nitrogen in both cases.¹⁰ However, while the chain extends along a two-fold axis in the previous case, the metal atom sits on an inversion center in U-AHA. The dihedral angle between the equatorial planes of successive uranyl ions along the chain is 27.90(8)°. The dihedral angle is measured between the mean plane defined by the six atoms around one uranyl ion and the mean plane

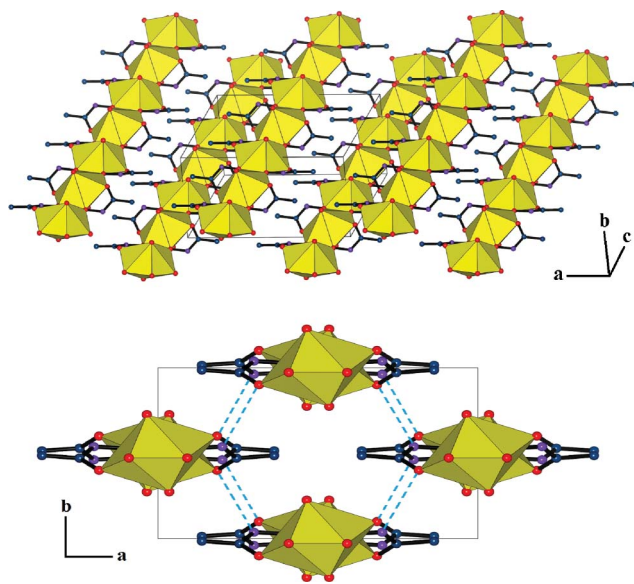


Fig. 2 Top: View of the packing of chains showing the uranium coordination polyhedra. Bottom: View of the packing down the *c*-axis with hydrogen bonds represented as dashed lines. Hydrogen atoms are omitted in both views. Color legend: U, yellow; O, red; N, purple; C, blue.

Table 1 Selected bond lengths (Å) and angles (°)^a

| Parameters ^a | Exp. | DFT |
|-------------------------|------------|-------|
| U–O1 | 1.766(5) | 1.80 |
| U–O2 | 2.432(5) | 2.46 |
| U–O3 | 2.519(5) | 2.55 |
| U–O3'' | 2.513(4) | 2.55 |
| O2–C1 | 1.288(8) | 1.29 |
| O3–N1 | 1.375(7) | 1.36 |
| N1–C1 | 1.300(9) | 1.31 |
| C1–C2 | 1.482(9) | 1.49 |
| O1–U–O1' | 180 | 180 |
| O2–U–O2' | 180 | 180 |
| O3–U–O3' | 180 | 180 |
| O2–U–O3 | 62.44(15) | 62.1 |
| O2–U–O3''' | 66.63(15) | 66.4 |
| O3–U–O3''' | 53.90(17) | 54.0 |
| O1–U–O2 | 86.0(2) | 86.7 |
| O1–U–O3 | 97.75(19) | 97.6 |
| O1–U–O3'' | 84.85(18) | 85.5 |
| C1–O2–U | 118.6(4) | 118.8 |
| N1–O3–U | 111.7(3) | 112.6 |
| N1''–O3''–U | 122.7(4) | 121.9 |
| U–O3–U'' | 125.11(17) | 125.2 |
| C1–N1–O3 | 119.1(6) | 119.5 |
| O2–C1–N1 | 117.6(6) | 118.1 |
| O2–C1–C2 | 122.5(6) | 122.5 |
| N1–C1–C2 | 119.8(6) | 119.4 |

^a Symmetry codes: ' = 1 - x, -y, 2 - z; '' = 1 - x, y, 5/2 - z; ''' = x, -y, z - 1/2.

defined by the six atoms around the neighboring uranyl ion. As expected, the U–O2 bond length, 2.432(5) Å, is smaller than the average bond length with the bridging O3 atoms, 2.516(3) Å, and these values match their counterparts in the other polymeric compound, 2.428(6) and 2.49(2) Å, respectively. Hydrogen bonds linking the protonated N1 atoms of one chain to the O2 atoms of a neighboring chain are present [N1...O2' 2.575(8), N1–H 0.88, H...O2' 2.02 Å, N1–H...O2' 120°; symmetry code ' = x, -y, z + 1/2] (*cf.* Fig. 2), while an intramolecular hydrogen bond involving the hydroxy substituent is formed in the 2-hydroxy-benzohydroxamate complex. Long-range interactions are also possibly present between the exterior methyl group and the -yl oxygen atoms, with an O1...H contact at 2.29 Å.

As shown in Table 1, structural parameters calculated using all-electron scalar relativistic density functional theory at the PW91/DNP level are in close agreement with experimental data, *i.e.* within less than 2% for bond lengths and less than 1% for bond angles. The relaxed unit-cell parameter along the polymeric chain direction is $c = 9.07$ Å, *i.e.* 1.5% larger than the experimental value. The axial uranium–oxo bonds in the polymeric chain (1.80 Å) are slightly elongated compared to the U=O distance in the isolated UO_2^{2+} ion which is predicted to be 1.72 Å at the same level of theory,¹² in excellent agreement with fully relativistic Dirac–Hartree–Fock results.¹³ The computed equatorial U–O distances also reproduce the experimental observation of a U–O2 bond length, 2.46 Å, smaller than the bond lengths with the bridging O3 atoms, 2.55 Å. The calculated dihedral angle between the equatorial planes of successive uranyl ions along the chain is 26.7°, *i.e.* 4.3% smaller than experiment. This large deviation, compared to other structural parameters, suggests that interchain forces, which are not accurately described with standard DFT, may play

a significant role in the relative orientation of adjacent uranium coordination polyhedra.

Chemical bonding and electronic structure

Partial atomic charges using the Hirshfeld partitioning of the electron density have also been computed.¹⁴ Hirshfeld charges provide a chemically accurate description of the interplay of charge redistribution and structural changes occurring in the vicinity of the actinide metal centers upon modification of their molecular environment.¹² The charge carried by U is +0.68 *e*, as a result of metal-to-ligand charge-transfer (MLCT) to the -yl O1 atoms (-0.28 *e*) and to the equatorial O2 (-0.19 *e*) and O3 (-0.17 *e*) atoms. The charge of N1 is essentially unchanged (-0.01 *e*), while C1 and C2 possess charges of +0.16 *e* and -0.11 *e*, respectively. This suggests that significant charge transfer occurs from C1 to O2. The protons of the methyl group and the hydroxamate ligand carry charges of +0.05 *e* and +0.11 *e*, respectively.

The computed band structure and the total and projected densities of states of the U-AHA crystal are displayed in Fig. 3. Calculations show that this polymeric compound is a semiconductor, with a direct gap of 1.1 eV opening at the center of the Brillouin zone (Γ point). This value is close to the energy band gap of monocrystalline Si, 1.11 eV,¹⁵ and lies near the gap energy for optimum solar-cell efficiency at room temperature.¹⁶ Therefore, this compound might be suitable for efficient polymer photovoltaics, similar to transition-metal oxide polymeric structures for solar-energy conversion.¹⁷

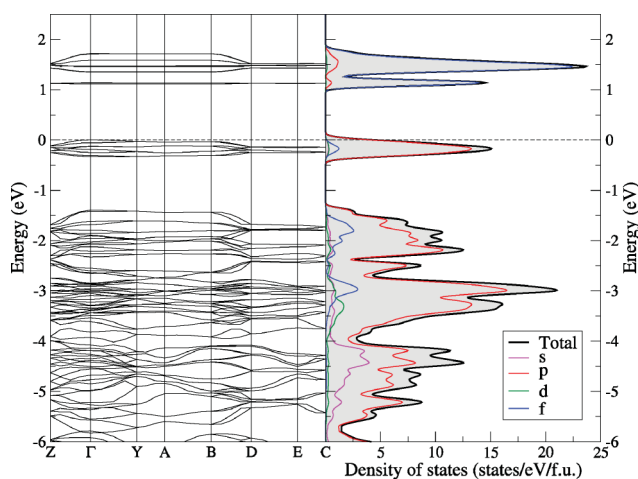


Fig. 3 Electronic band structure (left) and total and projected densities of states (right) of the U-AHA crystal. The Fermi energy is set to zero.

As shown in Fig. 3, 2p states dominate the top of the valence band, while states at the bottom of the conduction band are derived primarily from U 5f orbitals. 2p–5f hybridization occurs predominantly below *ca.* -1.5 eV. U 6d and U 7s orbitals only play a minor role close to the Fermi level but contribute more efficiently below -3.0 eV, with in particular a strong 2p–7s hybridization seen below -4.0 eV. The crystal orbitals corresponding to the lowest-energy conduction band and the highest-energy valence band at the Γ point are represented in Fig. 4. A close examination of these frontier orbitals reveals that the upper valence band is formed by 2p_x states isolated on the O1 and O3 atoms, as well as by π orbitals resulting from the constructive overlap of C1 and N1 2p_x orbitals

(the *z* axis is chosen here perpendicular to the U equatorial plane and the *y* axis along the chain propagation direction); although not shown in Fig. 4, non-bonding 2p_x orbitals of the -yl O atoms also contribute weakly to the upper valence band. The lower conduction band is essentially formed by 5f_{y(3x²-y²)} states.

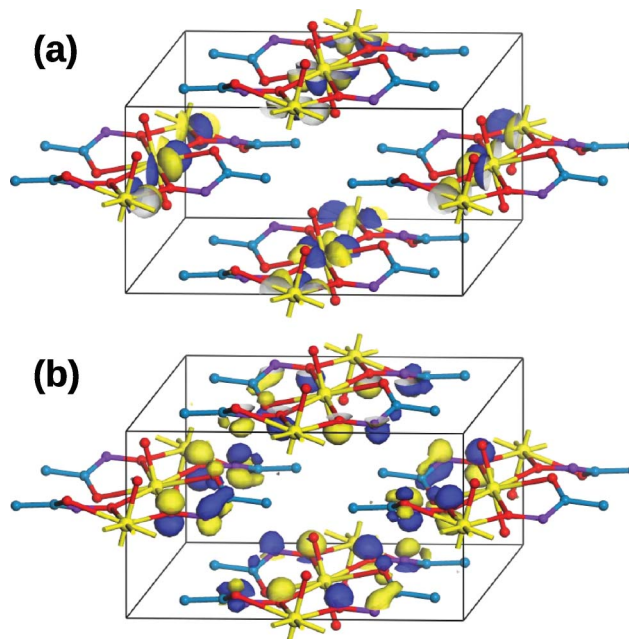


Fig. 4 Frontier crystal orbitals of U-AHA calculated at the GGA/PW91 level of theory. Crystal orbitals corresponding to (a) the lowest-energy conduction band and (b) the highest-energy valence band at the Γ point are represented with an isovalue of 0.03. The lower conduction band is essentially formed by 5f_{y(3x²-y²)} states. The upper valence band is formed by 2p_x states isolated on the O1 and O3 atoms, as well as by π orbitals resulting from the constructive overlap of C1 and N1 2p_x orbitals. The wavefunction phase is distinguished by yellow and blue colors. Hydrogen atoms are omitted in both views.

Conclusions

Using single crystal X-ray diffraction measurements and all-electron scalar relativistic DFT calculations, the structure of the uranyl-diacetohydroxamate compound, $\text{UO}_2(\text{C}_2\text{NO}_2\text{H}_4)_2$, was elucidated. This polymeric compound crystallizes in the $C2/c$ space group, with main-chain repeating units featuring a bidentate structure. DFT analysis reveals that metal-to-ligand charge-transfer occurs between U and the -yl and equatorial O atoms and that this compound is a semiconductor, with a direct gap of 1.1 eV. The modification of organic linkers between uranyl moieties should offer a viable means of tuning the band gap for specific device applications.

Experimental

Synthesis and purification

Powdered samples of 0.390 g uranyl acetate (The General Chemical Company) and 0.158 g AHA (Alfa Aesar) were manually ground together in an agate mortar until a sticky, dark orange paste was formed, after 15 min of vigorous grinding. This was

washed three times in cold acetone by batch resuspension and dried under gentle vacuum overnight for a final yield of 0.382 g (89%). The purity of all products was assessed *via* UV-vis, ¹H-NMR, and ATR-FT-IR spectroscopies.

Additional details of the synthesis and purification methods, as well as alternative methods of energy input and spectroscopic characterization of the products, can be found elsewhere.¹¹

Crystallography

A single crystal of U-AHA with dimensions of 15 μm × 35 μm, from a batch obtained as previously reported,¹¹ was mounted on a glass fiber and, by use of a digital camera, optically aligned on a Bruker APEX CCD X-ray diffractometer. Initial intensity measurements were performed using graphite monochromated Mo-Kα radiation from a sealed tube and monocapillary collimator. SMART¹⁸ was utilized for preliminary cell constant determinations and data collection control. The intensities of reflections of a sphere were collected by a combination of three sets of exposures (frames), each set consisting of 600 frames. Each set had a unique φ angle for the crystal and each exposure covered a range of 0.3° in ω. The exposure time per frame for the resulting 1800 frames was 30 s/frame. Determination of integrated intensities and global refinement were performed with the Bruker SAINT¹⁸ software package using a narrow-frame integration algorithm. These data were treated with a semi-empirical absorption correction by SADABS.¹⁸ The program suite SHELXTL (v 6.12) was used for space group determination (XPREP), direct methods structure solution (XS), and least-squares refinement (XL).¹⁹ The final refinements included anisotropic displacement parameters for all atoms. Secondary extinction was not noted, nor was there evidence of twinning. Crystal data and structure refinement details are given in Table 2. The drawings were done with SHELXTL¹⁹ and Vesta.²⁰

Table 2 Crystal data and structure refinement details

| Compound | U-AHA |
|--|---|
| Formula | C ₄ H ₈ N ₂ O ₆ U |
| Color and habit | Orange acicular prism |
| Crystal system | Monoclinic |
| Space group | C2/c (No. 15) |
| <i>a</i> (Å) | 12.8386(13) |
| <i>b</i> (Å) | 7.5661(7) |
| <i>c</i> (Å) | 8.9299(9) |
| β (°) | 103.185(2) |
| <i>V</i> (Å ³) | 844.57(14) |
| <i>Z</i> | 4 |
| ρ _c /g cm ⁻³ | 3.289 |
| μ (Mo-Kα) (cm ⁻¹) | 19.222 |
| <i>T</i> (K) | 193 |
| λ (Å) | 0.71073 |
| Maximum 2θ (°) | 56.63 |
| <i>R</i> _{int} | 0.044 |
| Reflections (total) | 4324 |
| Reflections (independent) | 4154 |
| Parameters | 61 |
| Δρ _{min} , Δρ _{max} (e Å ⁻³) | -0.80, 2.14 |
| <i>R</i> ₁ ^a for <i>F</i> _o ² > 2σ(<i>F</i> _o ²) | 0.023 |
| <i>wR</i> ₂ ^b | 0.059 |

^a $\sum ||F_o| - |F_c|| / |F_o|$. ^b $[\sum w(|F_o|^2 - |F_c|^2)|^2 / \sum w|F_o|^2]^{1/2}$ all reflections.

Computational methods

All-electron scalar relativistic calculations of the total energies, optimized geometries, and properties were performed using density functional theory as implemented in the DMol3 software.²¹ The exchange correlation energy was calculated using the generalized gradient approximation²² (GGA) with the parametrization of Perdew and Wang (PW91).²³ GGA functionals such as PW91 or PBE²⁴ are generally preferred over hybrid functionals which do not appear to describe bonds as accurately in actinide-bearing molecular systems.²⁵

Double numerical basis sets including polarization functions on all atoms (DNP) were used in the calculations. The DNP basis set corresponds to a double-ζ quality basis set with a p-type polarization function added to hydrogen and d-type polarization functions added to heavier atoms. For main-group elements, the DNP basis set is comparable to 6-31G** Gaussian basis sets²⁶ with a better accuracy for a similar basis set size.²¹ For the U atom, 5f, 6d and 7s polarization functions were added. In the generation of the numerical basis sets, a global orbital cutoff of 5.9 Å was used.

A supercell approach was used in the calculations to represent the 3D-periodic system, with a unit cell containing four formula units. The Brillouin zone was sampled using the Monkhorst–Pack special *k*-point scheme²⁷ with a 2 × 3 × 3 mesh for structural optimization and total energy calculations. The *c* unit-cell parameter along the polymeric chain direction was relaxed, while the *a* and *b* parameters were fixed to experimental values. These structural constraints were motivated by the fact that standard DFT, as used in this study, cannot account accurately for long-range intermolecular forces between adjacent chains. The energy tolerance in the self-consistent field calculations was set to 10⁻⁶ Hartree. Optimized geometries were obtained without symmetry constraints using the direct inversion in a subspace method (DIIS) with an energy convergence tolerance of 10⁻⁵ Hartree and a gradient convergence of 2 × 10⁻³ Hartree/Bohr.

The charge density was expressed by a nucleus-centered multipole expansion truncated at the octupole level. The spin–orbit coupling was neglected in the calculations as it is expected to be small in a strong ligand-field.

This computational approach has shown previously to yield accurate structural results and properties for molecular systems and compounds containing uranium and other f elements.^{12,28,29,30}

Acknowledgements

Funding for this research was provided by the US Department of Energy, Cooperative Agreement No. DE-FG07-01AL6735B. We gratefully acknowledge the assistance of Travis Bray at the early stage of this project.

References

- W. L. Leong and J. J. Vittal, *Chem. Rev.*, 2011, **111**, 688 and references therein.
- (a) C. L. Cahill, D. T. de Lill and M. Frisch, *CrystEngComm*, 2007, **9**, 15; (b) C. L. Cahill and L. A. Borkowski, in *Structural Chemistry of Inorganic Actinide Compounds*, S. V. Krivovichev, P. C. Burns and I. G. Tananaev, ed.; Elsevier: Amsterdam, Oxford, 2007; Chapter 11, pp 409–442.
- J. Leciejewicz, N. W. Alcock and T. J. Kemp, *Struct. Bonding*, 1995, **82**, 43.

- 4 See, for example: (a) Y. S. Jiang, Z. T. Yu, Z. L. Liao, G. H. Li and J. S. Chen, *Polyhedron*, 2006, **25**, 1359; (b) M. Frisch and C. L. Cahill, *Dalton Trans.*, 2006, 4679; (c) P. Thuéry, *Inorg. Chem.*, 2007, **46**, 2307; (d) B. Masci and P. Thuéry, *Cryst. Growth Des.*, 2008, **8**, 1689; (e) N. E. Dean, R. D. Hancock, C. L. Cahill and M. Frisch, *Inorg. Chem.*, 2008, **47**, 2000; (f) Z. L. Liao, G. D. Li, M. H. Bi and J. S. Chen, *Inorg. Chem.*, 2008, **47**, 4844; (g) C. Villiers, P. Thuéry and M. Ephritikhine, *Angew. Chem., Int. Ed.*, 2008, **47**, 5892; (h) C. Ji, J. Li, Y. Li and H. Zheng, *Inorg. Chem. Commun.*, 2010, **13**, 1340; (i) C. E. Rowland, N. Belai, K. E. Knope and C. L. Cahill, *Cryst. Growth Des.*, 2010, **10**, 1390; (j) J. A. Rusanova, E. B. Rusanov and K. V. Domasevitch, *Acta Crystallogr., Sect. C: Cryst. Struct. Commun.*, 2010, **66**, m207; (k) Y. Xia, K. X. Wang and J. S. Chen, *Inorg. Chem. Commun.*, 2010, **13**, 1542; (l) P. Thuéry, *Cryst. Growth Des.*, 2011, **11**, 347.
- 5 (a) A. N. Alsobrook, W. Zhan and T. E. Albrecht-Schmitt, *Inorg. Chem.*, 2008, **47**, 5177; (b) K. E. Knope and C. L. Cahill, *Inorg. Chem. Commun.*, 2010, **13**, 1040; (c) K. E. Knope and C. L. Cahill, *Eur. J. Inorg. Chem.*, 2010, 1177; (d) P. O. Adelani and T. E. Albrecht-Schmitt, *Inorg. Chem.*, 2010, **49**, 5701.
- 6 C. E. Rowland and C. L. Cahill, *Inorg. Chem.*, 2010, **49**, 8668.
- 7 F. H. Allen, *Acta Crystallogr., Sect. B: Struct. Sci.*, 2002, **58**, 380.
- 8 (a) W. L. Smith and K. N. Raymond, *J. Inorg. Nucl. Chem.*, 1979, **41**, 1431; (b) U. Casellato, P. A. Vigato, S. Tamburini, R. Graziani and M. Vidali, *Inorg. Chim. Acta*, 1984, **81**, 47; (c) S. Chakraborty, S. Dinda, R. Bhattacharyya and A. K. Mukherjee, *Z. Kristallogr.*, 2006, **221**, 606.
- 9 M. Hojjatie, S. Muralidharan, S. P. Bag, G. C. Panda and H. Freiser, *Iran J. Chem. Chem. Eng.*, 1995, **15**, 81.
- 10 R. Centore, G. De Tommaso, M. Iuliano and A. Tuzi, *Acta Crystallogr., Sect. C: Cryst. Struct. Commun.*, 2007, **63**, m253.
- 11 C.-M. S. Gong, F. Poineau and K. R. Czerwinski, *Radiochim. Acta*, 2007, **95**, 439.
- 12 P. F. Weck, E. Kim, B. Masci, P. Thuéry and K. R. Czerwinski, *Inorg. Chem.*, 2010, **49**, 1465.
- 13 W. A. de Jong, R. J. Harrison, J. A. Nichols and D. A. Dixon, *Theor. Chem. Acc.*, 2001, **107**, 22.
- 14 F. L. Hirshfeld, *Theor. Chim. Acta*, 1977, **44**, 129.
- 15 B. G. Streetman and S. Banerjee, *Solid State electronic Devices*, 5th ed., Prentice Hall, New Jersey, 2000.
- 16 S. M. Sze, *Semiconductor Devices-Physics and Technology*, Wiley, New York, 1985.
- 17 A. C. Arango, L. R. Johnson, V. N. Bliznyuk, Z. Schlesinger, S. A. Carter and H.-H. Hörhold, *Adv. Mater.*, 2000, **12**, 1689.
- 18 Bruker (2001). SMART (Version 5.624), SAINT (Version 6.02) and SADABS. Bruker AXS Inc., Madison, Wisconsin, USA.
- 19 G. M. Sheldrick, *Acta Crystallogr., Sect. A: Found. Crystallogr.*, 2008, **64**, 112.
- 20 K. Momma and F. Izumi, *J. Appl. Crystallogr.*, 2008, **41**, 653.
- 21 B. Delley, *J. Chem. Phys.*, 2000, **113**, 7756.
- 22 J. P. Perdew, *Phys. Rev. B*, 1986, **33**, 8822.
- 23 Y. Wang and J. P. Perdew, *Phys. Rev. B*, 1991, **44**, 13298.
- 24 J. P. Perdew, J. Burke and M. Ernzerhof, *Phys. Rev. Lett.*, 1996, **77**, 3865.
- 25 G. A. Shamov, G. Schreckenbach, R. L. Martin and P. J. Hay, *Inorg. Chem.*, 2008, **47**, 1465.
- 26 W. J. Hehre, L. Radom, P. R. Schleyer and J. A. Pople, *Ab Initio Molecular Orbital Theory*, Wiley, New York, 1986.
- 27 H. J. Monkhorst and J. D. Pack, *Phys. Rev. B*, 1976, **13**, 5188.
- 28 P. F. Weck, E. Kim, N. Balakrishnan, F. Poineau, C. B. Yeaman and K. R. Czerwinski, *Chem. Phys. Lett.*, 2007, **443**, 82.
- 29 J. Warburton, P. F. Weck, N. Smith and K. R. Czerwinski, *J. Nucl. Mater. Manag.*, 2010, **39**, 26.
- 30 P. F. Weck, E. Kim, F. Poineau, E. E. Rodriguez, A. P. Sattelberger and K. R. Czerwinski, *Dalton Trans.*, 2010, **39**, 7207.